Supplemental File for

Melting and melt segregation processes controlling granitic melt composition

Yang Yu [a,b], Xiao-Long Huang [a,b*], Roberto F. Weinberg [c], Min Sun [d], Peng-Li He [a,b], Le Zhang [a]

[a] State Key Laboratory of Isotope Geochemistry, CAS Center for Excellence in Deep Earth Science, Guangzhou Institute of Geochemistry, Chinese Academy of Sciences, Guangzhou 510640, China

[b] Southern Marine Science and Engineering Guangdong Laboratory (Guangzhou), Guangzhou 511458, China

[c] School of Earth, Atmosphere and Environment, Monash University, Clayton, VIC 3800, Australia

[d] Department of Earth Sciences, The University of Hong Kong, Pokfulam Road, Hong Kong

Contents of this file

1. Detailed analytical methods

Zircons from the melanosome and net-structured leucosome were selected for U-Pb age and trace elements, which were determined by laser ablation inductively coupled plasma mass spectrometry (LA-ICP-MS) (Resonetics RESOlution S-155 laser + Agilent 7900) with a spot size of 29 μm and a laser frequency of 8 Hz. Each analysis included approximately 20–30 s of back-ground acquisition (from a gas blank) followed by 50 s of

data acquisition from the sample. U-Pb age of zircon was calibrated by standard zircon 91500 and Plesovice. The standard NIST610 was adopted as external calibration reference and Si was used as the internal standard to quantify elemental concentrations in samples. The off-line selection and integration of the background and analytical signals, time-drift correction and quantitative calibration, were performed using ICPMSDataCal (Lin et al., 2016; Liu et al., 2008). The uncertainties of individual analyses are reported at the 1σ level, and the data reduction was carried out using Isoplot/Ex 3 software (Ludwig, 2003).

Back-scattered-electron (BSE) images and X-ray mappings were obtained using a Carl Zeiss SUPRA55SAPPHIRE Field Emission-Scanning Electron Microscope (SEM). In situ major elemental composition of minerals were analyzed using a Cameca SXFive FE Electron Probe Microanalyzer (EPMA). The operating conditions are: 15 kV accelerating voltage, 20 nA beam current, 5 μm beam diameter with peak counting time varying from 8 s to 40 s depending on the intensity of characteristic X-ray line and desired precision. The matrix correction is based on the PAP (Pouchou and Pichoir) procedure (Pouchou and Pichoir, 1991). In situ trace elemental analyses of minerals were conducted with an ELEMENT XR (Thermo Fisher Scientific) ICP-SF-MS coupled with a 193-nm (ArF) Resonetics RESOlution M-50 laser ablation system. Laser conditions were set as following: beam size, 45 μm; repetition rate, 5 Hz; energy density, ~4 J cm^{-2}. The calibration line for each element was constructed by analyzing three USGS reference glasses BCR-2G, BHVO-2G and GSD-1G with Si or Ca as an internal standard. The USGS reference glass TB-1G was measured as unknown samples. Repeated analyses of TB-1G indicate that both precision and accuracy are better than 5 % for most elements.

In situ Nd isotope analyses of apatite were performed on a Neptune Plus MC-ICP-MS (Thermo Scientific), coupled with a RESOlution M-50 193 nm laser ablation system (Resonetics). The detailed data reduction procedure is reported in Zhang et al. (2015). The laser parameters were set as follow: beam diameter, 112 μm; repetition rate, 8 Hz; energy density, ~4 $J \cdot cm^{-2}$. Helium was chosen as the carrier gas (800 ml/min). Eight analyses of apatite McClure and 10 analyses of apatite Durango during the course of this study yielded a weighted mean of $^{143}Nd/^{144}Nd = 0.512224 \pm 0.000027$ (2SD) and $^{143}Nd/^{144}Nd = 0.512488 \pm 0.000021$ (2SD), respectively, which are consistent within errors with the reported ratios of 0.512246 ± 0.000080 for McClure and of 0.512472 ± 0.000046 for Durango (Yang et al., 2014).

Whole-rock major elements were determined by employing a Thermo Fisher ARL Perform'X 4200 X-ray fluorescence spectrometer (XRF) with analytical uncertainties between 1% and 5%. Trace element analysis was conducted by Thermal Fisher iCAP RQ ICP-MS equipped with a Cetac ASX-560 AutoSampler. The rock powder (~50 mg) was weighted into high-pressure Teflon vessels and dissolved with double distilled concentrated HNO_3-HF mixture. The sample solution was finally diluted to 4000 times with 2% HNO_3 and added with 6 ppb Rh, In, Re and Bi internal standard. USGS standards W-2a and BHVO-2 were used as reference standard. Instrument drift mass bias was corrected with internal standard and external monitors. Analytical precision of the REE and other incompatible element analyses is typically 1–5 %.

Whole-rock Nd isotopic compositions were determined on a subset of whole-rock sample powder by employing a Neptune plus MC-ICP-MS. Detailed procedures of sample preparation and chemical separation are same as those described by Liang et al. (2003).

The procedure blanks were ≤50 pg for Nd. The REE were separated using the cation exchange columns, and the Nd fractions were further separated by HDEHP-coated Kef columns. Measured $^{143}Nd/^{144}Nd$ ratios were normalized to $^{146}Nd/^{144}Nd = 0.7219$. Reference standard BHVO-2 was analyzed along with the unknowns, yielding $^{143}Nd/^{144}Nd$ ratio of 0.512974 ± 7 (2S), comparable to the recommended $^{143}Nd/^{144}Nd$ (0.512979 ± 14) ratios (Jochum et al., 2016).

Supplemental Figures S1 to S8

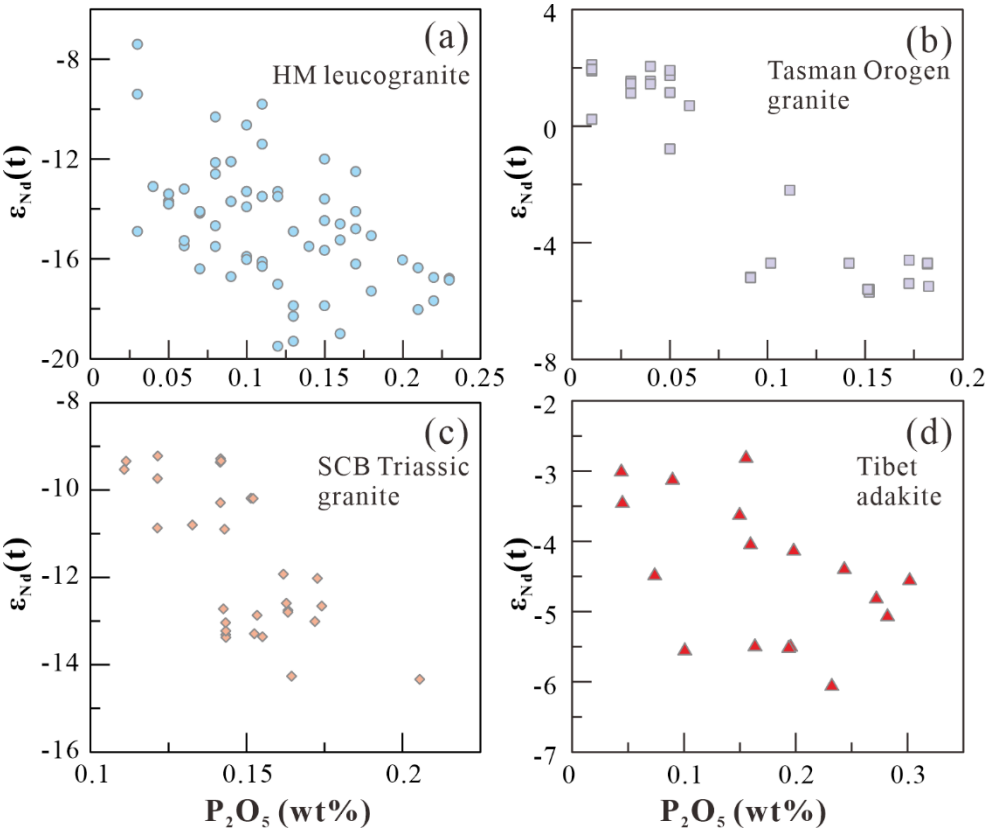

Fig. S1 $\varepsilon_{Nd}(t)$ vs. P_2O_5 for (a) the Himalayan leucogranites, (b) the Middle Paleozoic granite in the Tasman Orogen, (c) the Triassic granites in the South China Block (SCB), and (d) adakite in Tibet. Data sources of the Himalayan leucogranites, Triassic granites from the Guangxi province in the South China Block and Middle Paleozoic granites in the Tasman Orogen are same with Fig. 9. Data sources of the Tibet adakites same with Fig. 11.

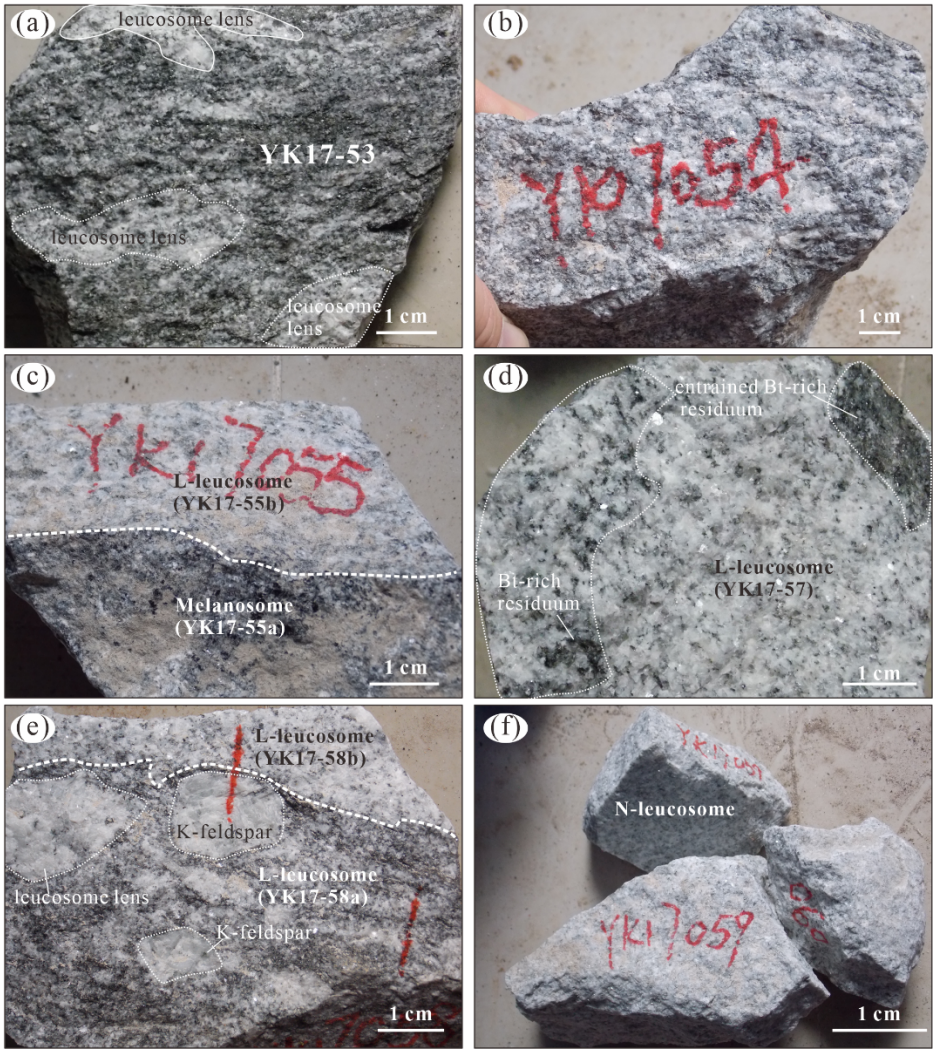

Fig. S2 Photographs showing some samples in this study: (a) leucosome lenses in the melanosome (YK17-53); (b) melanosome (YK17-54); (c) the relationship between lenticular (L) leucosome (YK17-55b) and biotite-rich residuum (YK17-55a); (d) entrained biotite-rich residuum in lenticular (L) leucosome (YK17-57b); (e) the relationship between lenticular (L) leucosome (YK17-58b) and melanosome sample (YK17-58a); and (f) representative sample of net-structured (N) leucosome (YK17-59 and YK17-60). Leucosome lenses and coarse-grained K-feldspars in melanosome and entrained residuum in leucosome, which is circled by white dot lines, had been cut off before powdered for whole-rock geochemical analyses.

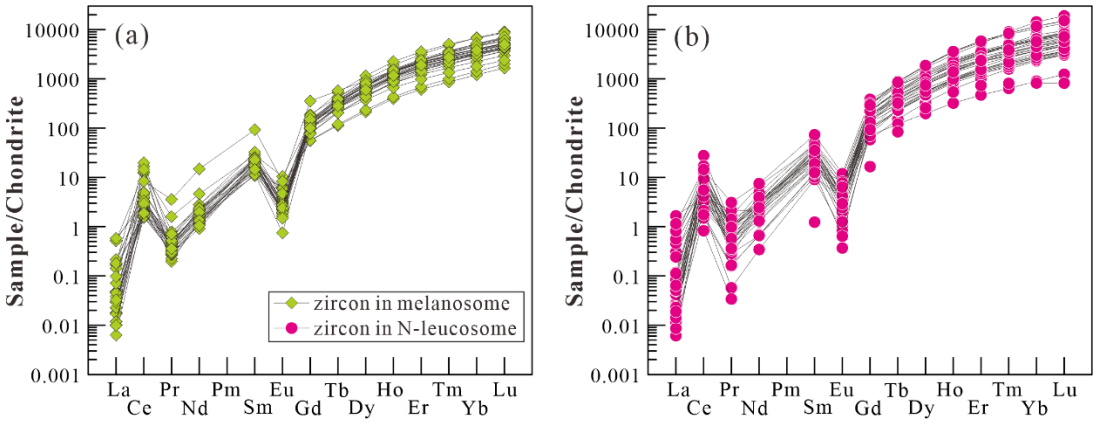

Fig. S3 Chondrite-normalized REE patterns of zircon from the (a) Jindong melanosome (YK17-56) and (b) net-structured leucosome (YK17-59).

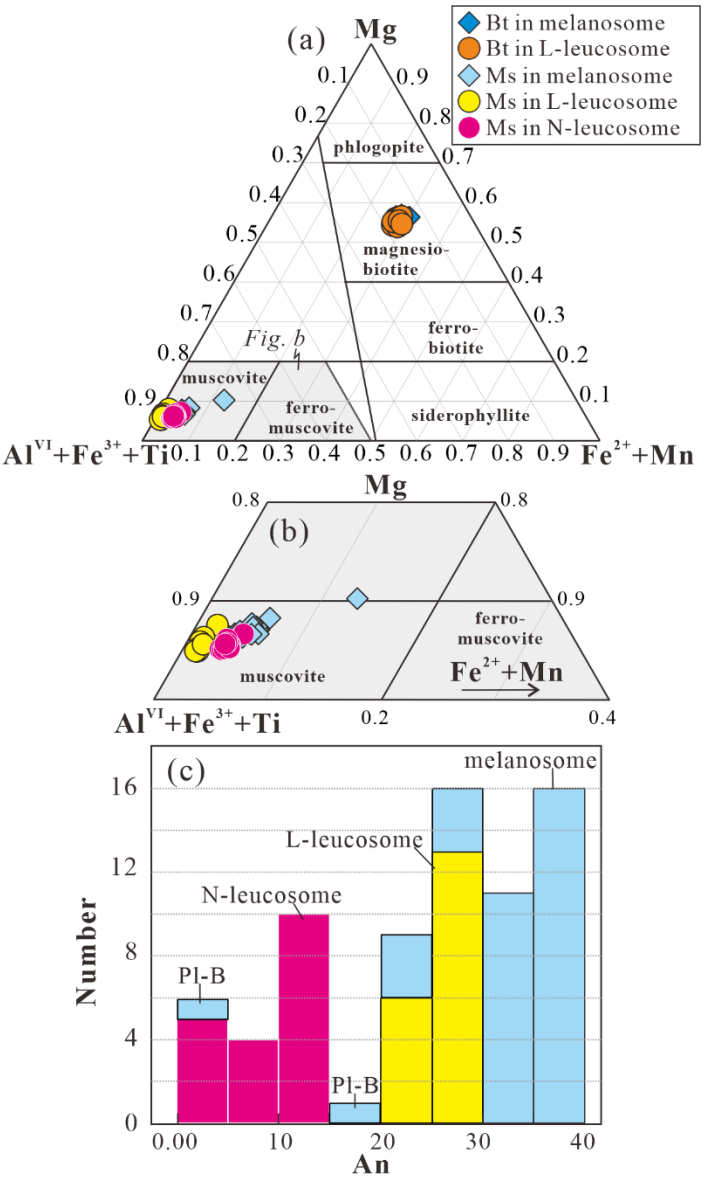

Fig. S4 Nomenclature of biotite (after Föster, 1960) and bar graph chart for An number of plagioclase in the Jindong melanosome, lenticular (L) leucosome and net-structured (N) leucosome. Pl-B refers plagioclase occur along biotite during retrogression reaction in the Jindong melanosome. Bt = biotite; Ms = muscovite; Pl = plagioclase.

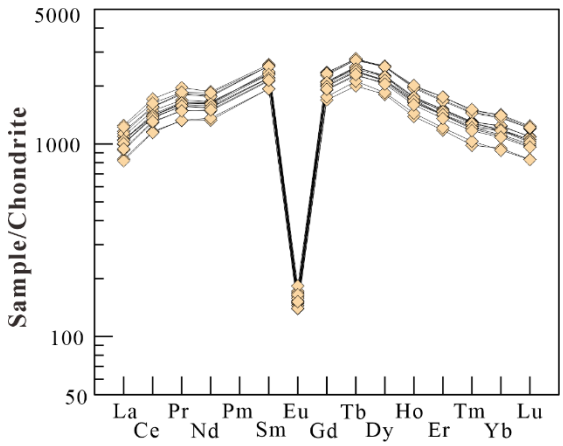

Fig. S5 Chondrite-normalized REE patterns of apatite from the Jindong melanosome (YK17-56).

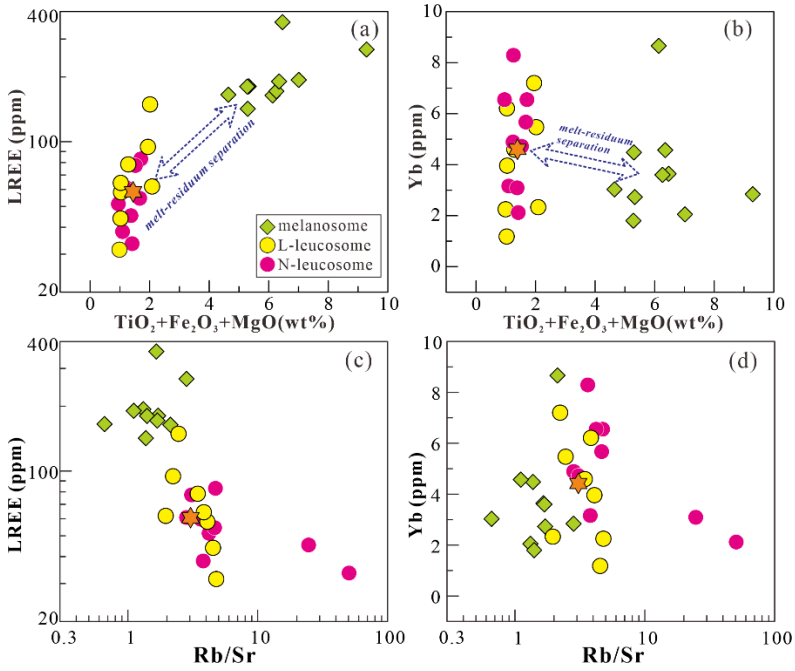

Fig. S6 Diagrams of (a) LREE vs. TiO_2 +Fe_2O_3 +MgO; (b) Yb vs. TiO_2 +Fe_2O_3 +MgO; (c) LREE vs. Rb/Sr and (d) Yb vs. Rb/Sr for the Jindong melanosome, lenticular (L) leucosome and net-structured (N) leucosomes. The orange star symbol represents average composition of lenticular leucosomes.

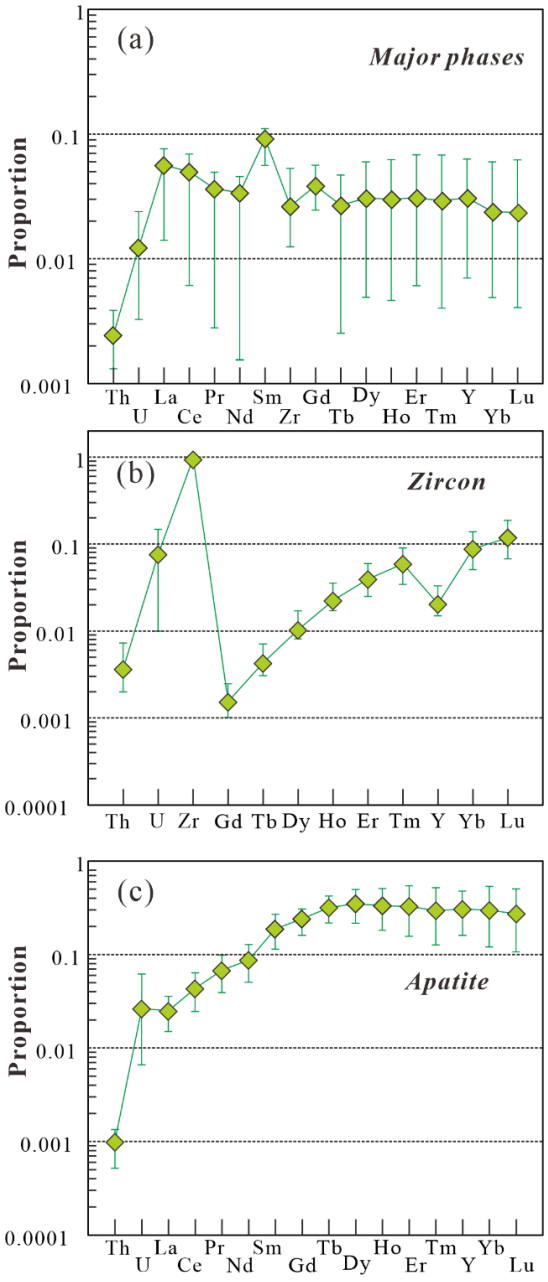

Fig. S7 Diagrams of (a)-(c) trace element budget of major phases, zircon and apatite in the Jindong gneissic granite, which is calculated based on mineral norm in Supplemental Table A1 and mineral compositions in Table A6.

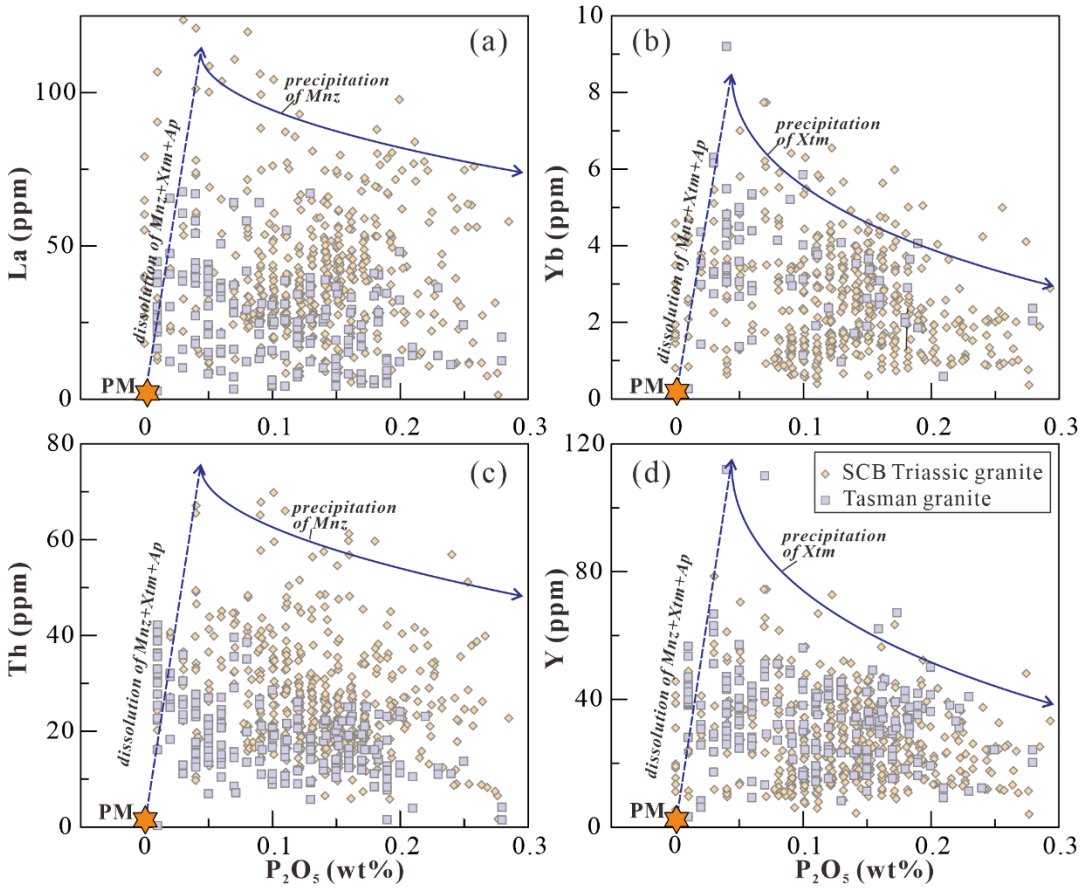

Fig. S8 (a) La vs. P_2O_5; (b) Yb vs. P_2O_5; (c) Th vs. P_2O_5 and (d) Y vs. P_2O_5 for the Triassic granite in the South China Block (SCB) and Middle Paleozoic granite from the Tasman Orogen. The dotted lines represent dissolution of "monazite (Mnz) + xenotime (Xtm) + apatite (Ap)", with assemblage of assemblage of 45%Ap + 0.19%Xtm + 36%Mnz, respectively. The trends marking the precipitation of monazite and xenotime with increasing P_2O_5 content in melts are represented by the dark blue lines and calculated based on Eq. 3, with precipitation of 0.0034%Mnz + 0.0041%Xtm as 1%Ap dissolution. The trends of apatite dissolution are calculated based on average composition of apatite (Table A6). Data sources of the Tasman Orogen granites and Triassic granites from the South China Block (SCB) are same with Fig. 9. The primitive melts (PM) represent melts formed through breakdown of major minerals, which were calculated based on the melting reaction Eq. 2 and average composition of major phases with $\varepsilon_{Nd}(t)$ value of -9.6.

References:

Föster, M.D., (1960) Interpretation of composition of trioctahedral micas. U. S. Geological Survey Professional Paper 354B, 1–49.

Jochum, K.P., Weis, U., Schwager, B., Stoll, B., Wilson, S.A., Haug, G.H., Andreae, M. O., and Enzweiler, J. (2016) Reference Values Following ISO Guidelines for Frequently Requested Rock Reference Materials. Geostandards and Geoanalytical Research, 40(3), 333–350.

Liang, X.R., Wei, G.J., Li, X.H., and Liu, Y. (2003) Precise measurement of $^{143}Nd/^{144}Nd$ and Sm/Nd ratios using multiple-collectors inductively couple plasma-mass spectrometer (MC-ICP-MS). Geochimica, 32, 91–96 (in Chinese with English abstract).

Lin, J., Liu, Y.S., Yang, Y.H., and Hu, Z.C. (2016) Calibration and correction of LA-ICP-MS and LA-MC-ICP-MS analyses for element contents and isotopic ratios. Solid Earth Sciences.1 (1), 5–27.

Liu, Y.S., Hu, Z.C., Gao, S., Gunther, D., Xu, J., Gao, C.G., and Chen, H.H. (2008) In situ analysis of major and trace elements of anhydrous minerals by LA-ICP-MS without applying an internal standard. Chemical Geology, 257 (1–2), 34–43.

Ludwig, K.R. (2003) Isoplot: a geochronological toolkit for Microsoft Excel. Berkeley Geochronology Center Special Publications. 4, 1–67.

Pouchou, J.L., and Pichoir, F. (1991) Quantitative Analysis of Homogeneous or Stratified Microvolumes Applying the Model "PAP". In: Heinrich, K.F.J., Newbury, D.E. (Eds), Electron Probe Quantification, Plenum Press, New York, pp. 31–75.

Yang, Y., Wu, F.F., Yang, J.H., Chew, D.M., Xie, L.W., Chu, Z., Zhang, Y., and Huang C. (2014) Sr and Nd isotopic compositions of apatite reference materials used in U–Th–Pb geochronology. Chemical Geology 385, 35–55.

Zhang, L., Ren, Z.Y., Xia, X.P., Li, J., and Zhang Z.F. (2015) IsotopeMaker: A Matlab program for isotopic data reduction. International Journal of Mass Spectrometry, 392, 118–124.